Efficient Complex Continuous-Time IIR Filter Design via Generalized Vector Fitting

Chi-Un Lei, Chung-Man Cheung, Hing-Kit Kwan and Ngai Wong *

Abstract—**We present a novel model identification technique for designing complex infinite-impulse-response (IIR) continuous-time filters through generalizing the Vector Fitting (VF) algorithm, which is extensively used for continuous-time frequency-domain rational approximation to symmetric functions, to asymmetrical cases. VF involves a two-step pole refinement process based on a linear least-squares solve and an eigenvalue problem. The proposed algorithm has lower complexity than conventional schemes by designing complex continuous-time filters *directly*. Numerical examples demonstrate that VF achieves highly efficient and accurate approximation to arbitrary asymmetric complex filter responses. The promising results can be realized for high-dynamic frequency range networks.**

Keywords: Complex filter, Vector Fitting, Rational Function Approximation

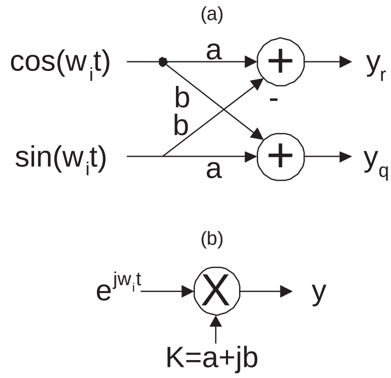

Figure 1: (a) The real signal-flow graph (SFG) of a complex multiply and (b) the equivalent complex SFG.

1 Introduction

Complex signal processing has growing importance in high-speed communication systems [1, 2]. This can be seen, for example, by the majority of the LAN wireless transceivers papers in IEEE International Solid-State Circuits Conference (2001-2003) and recent papers [3, 4]. The topology of a complex signal processing block comprises two parallel paths, namely, an in-phase path and a quadrature path. The two cross-coupling paths have equal magnitude gain but have $\pi/2$ phase difference, as in Fig. 1. Modern wireless systems make use of this property in the design of quadrature receivers for image rejection in intermediate frequency (IF), and suppression of out-of-band signals and interferences [1]. This paper revisits and explores the design of complex continuous-time filters.

Existing complex infinite-impulse-response (IIR) continuous-time filter design algorithms include the first-order frequency transformation of a real lowpass filter [5], which usually results in a high-order filter due to unnecessary coefficient symmetry. In [2] and [6], algorithms are proposed to combine real filter design and conformal mapping to eliminate such transformation. However, both methods can only approximate a single passband response (but not arbitrary, say, multiple passband response) and do not consider phase matching and efficient design for advanced and adaptive applications.

On the other hand, a continuous-time frequency-domain system identification technique, known as Vector Fitting (VF) [7], is a robust macromodeling tool for fitting sampled frequency data with a rational function. Its extensive applications include power system modelling [8] and high-speed VLSI interconnect simulations [9]. Its counterpart, called discrete-time vector fitting (VFz), has been adapted to real digital filter design in [10] with remarkable performance. However, traditional VF has been restricted to symmetric functions. In this paper, VF is adapted to asymmetric functions for complex IIR continuous-time filter design.

The core of VF is a two-step process for refining the filter poles such that the prescribed response can be accurately reproduced with only a low-order rational function. VF enjoys simple coding and guarantees well-conditioned arithmetic by means of partial fraction basis. Flipping of unstable poles ensures system stability. Numerical examples then confirm the efficacy and accuracy of VF in complex IIR filter design over conventional schemes, especially in the high dynamic frequency range.

*Department of Electrical and Electronic Engineering, The University of Hong Kong, Pokfulam Road, Hong Kong. Email: {culei, edmondcheung, kwanhk, nwong}@eee.hku.hk

ISBN: 978-988-17012-1-3

2 Vector Fitting

In complex filter design, the ultimate goal is to approximate a prescribed asymmetric frequency-domain response by a complex transfer function:

$$f(s) = H_0 \frac{\prod_{i=1}^{M}(s-\beta_i)}{\prod_{i=1}^{N}(s-\alpha_i)}, \tag{1}$$

where $H_0 \in \Re$ and $\alpha_i, \beta_i \in \mathbb{C}$. $f(s)$ is the desired frequency response, H_0, α_i, β_i, M and N represent gain, poles, zeros, the number of zeros and the number of poles, respectively.

To fit the continuous-time rational function, Vector Fitting (VF) [7] attempts to reformulate (1) into partial fraction basis:

$$f(s) = (\sum_{n=1}^{N} \frac{c_n}{s-a_n}) + d + se, \tag{2}$$

to a set of calculated/sampled data points at frequencies $\{s_k\}$, for $k = 1, 2, \cdots, N_s$. In real response approximation of VF, the poles a_n and residues c_n are real or complex conjugate pairs. In complex filtering, this restriction is relaxed and VF readily handles complex poles and zeros arising in this stage. The constant term d and e are generally complex.

2.1 Problem Formulation

The fitting process begins with specifying an initial set of pole $\{\alpha_n^{(0)}\}$. By introducing of the scaling function $\sigma(s)$, a linear problem is set up for the ith iteration, namely

$$\underbrace{\left(\sum_{n=1}^{N} \frac{c_n}{s-\alpha_n^{(i)}}\right) + d + se}_{(\sigma f)(s)} \approx \underbrace{\left(\left(\sum_{n=1}^{N} \frac{\gamma_n}{s-\alpha_n^{(i)}}\right) + 1\right)}_{\sigma(s)} f(s), \tag{3}$$

for $i = 0, 1, \cdots, N_T$, where N_T denotes the number of iterations when convergence is attained or when the upper limit is reached. The unknowns, c_n, d, e and γ_n, are solved through an overdetermined linear equation formed by evaluating (3) at the N_s sampled frequency points. One important feature in (3) is that $(\sigma f)(s)$ and $\sigma(s)f(s)$ are enforced to share the same set of poles, which in turn implies that the original poles of $f(s)$ are cancelled by the zeros of $\sigma(s)$. And the relationship can be described as follows:

$$\underbrace{\frac{\prod_{n=1}^{N+1}\left(s-\beta_n^{(i)}\right)}{\prod_{n=1}^{N}\left(s-\alpha_n^{(i)}\right)}}_{(\sigma f)(s)} \approx \underbrace{\frac{\prod_{n=1}^{N+1}\left(s-\widetilde{\beta}_n^{(i)}\right)}{\prod_{n=1}^{N}\left(s-\alpha_n^{(i)}\right)}}_{\sigma(s)} f(s), \tag{4}$$

$$\Rightarrow f(s) \approx \frac{(\sigma f)(s)}{\sigma(s)} = \frac{\prod_{n=1}^{N+1}\left(s-\beta_n^{(i)}\right)}{\prod_{n=1}^{N+1}\left(s-\widetilde{\beta}_n^{(i)}\right)}. \tag{5}$$

Subsequently, solving the zeros of $\sigma(s)$, in the least-squares sense, results in an approximation to the poles of $f(s)$, i.e., $\{\alpha_n^{(i+1)}\}$, without restriction of real coefficients. The new poles are then fed back to (3) as the next set of known poles for further refinement iteratively. In practical implementation, the fitting equation in (3) is linear in its unknowns c_n, d and γ_n. Therefore, the non-linear problem can be solved using over-determined equations and eigenvalue solving.

2.2 Pole Calculation

At a particular frequency point, with $e = 0$, (3) becomes

$$\left(\sum_{n=1}^{N} \frac{c_n}{s_k-\alpha_n^{(i)}}\right) + d - \left(\sum_{n=1}^{N} \frac{\gamma_n f(s_k)}{s_k-\alpha_n^{(i)}}\right) \approx f(s_k), \tag{6}$$

it can be reformulated into:

$$A_k x = b_k, \tag{7}$$

where $x = \begin{bmatrix} c_1 & \cdots & c_N & 1 & \gamma_1 & \cdots & \gamma_N \end{bmatrix}^T$, $A_k = \begin{bmatrix} \frac{1}{s_k-\alpha_1^{(i)}} & \cdots & \frac{1}{s_k-\alpha_N^{(i)}} & d & \frac{-f(s_k)}{s_k-\alpha_1^{(i)}} & \cdots & \frac{-f(s_k)}{s_k-\alpha_N^{(i)}} \end{bmatrix}$ and $b_k = f(s_k)$.

In the above expression, A_k and x are row and column vectors, respectively, while b_k is a scalar.

Equating (7) at all frequency samples, mathematically $s_k = j\Omega_k$, for $k = 1, 2, \cdots, N_S$, where $N_S > 2N + 1$, and by stacking A_k's and b_k's into a (tall) column matrix and a vector, an overdetermined equation for the ith iteration is obtained:

$$Ax = b. \tag{8}$$

The scaling function $\sigma(s)$ in (3) can be reconstructed from the last N entries obtained from the least-squares solution (i.e., γ_1,γ_2,$\cdots$,γ_N in x), such that its zeros, $\{\alpha_n^{(i+1)}\}$, for $n = 1, 2, \cdots, N$, are taken as the new set of starting poles in the next VF iteration. Moreover, it can be shown that $\{\alpha_n^{(i+1)}\}$ are conveniently computed as the eigenvalues of $\Psi \in \mathbb{C}^{N\times N}$ where

$$\Psi = \begin{bmatrix} \alpha_1^{(i)} & & & \\ & \alpha_2^{(i)} & & \\ & & \ddots & \\ & & & \alpha_N^{(i)} \end{bmatrix} - \begin{bmatrix} 1 \\ 1 \\ \vdots \\ 1 \end{bmatrix} \begin{bmatrix} \gamma_1 & \gamma_2 & \cdots & \gamma_N \end{bmatrix}. \tag{9}$$

Since the poles are not restricted to complex-conjugate pairs, Ψ is generally a complex matrix. Upon convergence, the update in $\alpha_n^{(i)}$ diminishes and $\sigma(s) \approx 1$.

To ensure system stability, it is necessary that $Re\left(\alpha_n^{(i+1)}\right) < 0$. If this is not the case, any unstable pole is flipped about the imaginary axis to the open left half plane $Re\left|\alpha_n^{(i+1)}\right| := -Re\left|\alpha_n^{(i+1)}\right|$. Such stability enforcement has the physical meaning of multiplying all-pass filters onto the filter transfer function such that the magnitude response is preserved.

2.3 Building the Rational Function

Once a converged set of poles $\{\alpha_n^{(N_T)}\}$ is obtained, the final stage is to reconstruct the rational function complex IIR filter. Referring to (3), we should now have $\sigma(s) \approx 1$ so that

$$\left(\sum_{n=1}^{N} \frac{c_n}{s - \alpha_n^{(N_T)}}\right) + d \approx f(s_k), \tag{10}$$

for $k = 1, 2, \cdots, N_s$. The residues c_n of $F(s)$ are determined exactly in the same manner, except (7) is replaced as follows:

$$A_k x = b_k, \tag{11}$$

where $x = \begin{bmatrix} c_1 & \cdots & c_N & 1 \end{bmatrix}^T$, $b_k = f(s_k)$ and $A_k = \begin{bmatrix} \frac{1}{s_k - \alpha_1^{(i)}} & \cdots & \frac{1}{s_k - \alpha_N^{(i)}} & d \end{bmatrix}$. The summation of partial fractions $\left(\sum\limits_{n=1}^{N} \frac{c_n}{s - \alpha_n^{(N_T)}}\right) + d$ generates a rational function representing the complex IIR filter in the form of (2). By seeking a near-optimal fit to $f(s_k)$ [5], VF matches both magnitude and phase of $f(s_k)$ simultaneously.

In summary, comparing to VF, other complex IIR design algorithms such as the pole-placement algorithm in [2] give similiar accuracy but has much higher computational requirement and does not emphasize the importance of phase linearity. For high-order filter design, it was claimed that 10-15 seconds are required on a 3-GHz computer [2], in great contrast to the 1-2 seconds by our design methodology implemented on a 1.8-GHz computer. In comparison to [2] and other complex filter design algorithms, VF is superior in terms of the phase linearity in passband and much higher efficiency, as will be seen in our numerical examples.

3 Remarks

3.1 Numerical consideration

Recent research has shown that VF is in fact a reformulation of the Sanathanan-Koerner (SK) iteration [11], an iterative continuous-time frequency-domain system identification technique [12], which minimizes the following objective function:

$$\begin{aligned} &\sum_{k=0}^{N_s} \left| \frac{N^{(i)}(s_k)}{D^{(i-1)}(s_k)} - \frac{D^{(i)}(s_k)}{D^{(i-1)}(s_k)} f(s_k) \right|^2 \\ &= \sum_{k=0}^{N_s} \left| \sum_{n=1}^{N} \frac{c_n}{s_k + \alpha_n^{(i-1)}} - \left(1 + \sum_{n=1}^{N} \frac{\gamma_n}{s_k + \alpha_n^{(i-1)}}\right) f(s_k) \right|^2, \end{aligned} \tag{12}$$

where $N^{(i)}$, $D^{(i)}$ are the numerator and denominator determined during the ith iteration. In theory, the approximation converges for a noise-free model using (12), but some numerical errors occur during iterative calculation [15]. Therefore, numerical considerations for improving the approximation accuracy are highlighted:

1. The approximation accuracy in noisy environment (e.g., finite precision) is affected by the equation normalization in the original VF. Furthermore, the normalization also gives a biased approximation in the low frequency region [13]. Recently, a relaxation is proposed to improve the normalization situation. Firstly, the unity basis in (3) is replaced by a variable and a relaxation constraint,

$$Re\left\{\sum_{k=0}^{N_s}\left(1 + \sum_{n=1}^{N} \frac{\gamma_n}{s_k + \alpha_n^{(i)}}\right)\right\} = N_s + 1, \tag{13}$$

   is introduced in (8) with a row weighting of $\|f(s)\|/(N_s+1)$. As shown in [14], this relaxation outperforms other relaxation approaches.

2. The conditioning and the approximant accuracy are affected by the choices of function basis and the location of initial-poles (i.e. $\alpha_n^{(0)}$ in (3)). In [7], it is recommended that the initial poles should be distributed over the frequency range of interest. As a rule of thumb in VF, the complex design algorithm starts with complex conjugate poles based on the following relationship:

$$a_n = -\alpha + j\beta, a_{n+1} = -\alpha - j\beta, \tag{14}$$

   where $\beta = 100\alpha$, α and β are the real part and the imaginary part of the initial poles, respectively. This selection criterion excludes the possibility of ill-conditioned computation in most practical cases.

   This problem can also be alleviated by introducing orthonormal function basis [15] or digital partial fraction basis [16]. In this paper, column scaling

Table 1: Approximation errors in the numerical examples.

	Ex 1. (VF)	Ex 1. ([2])	Ex. 2
L_2 passband	0.0124	0.0234	0.0083
L_∞ passband	0.0071	0.0126	0.0022
L_2 stopband	0.9975	1.0000	0.0068
L_∞ stopband	5.1452	5.1953	0.0029

technique from linear algebra [17] is used in system equation calculation to improve the numerical conditioning, and gives a similar accuracy as using the orthonormal basis.

3.2 Further extension

Besides L_2 norm minimization, some filter design requires equiripple passband to minimize the maximum error of a filter. In IIR digital filter design, an equiripple filter can be designed by a weighted least-squares method with a suitable least-squares frequency response weighting function [18]. The idea can be extended into complex filter design, and the frequency weighting can be included using row weighting in a particular frequency-data row of (7).

4 Numerical Examples

The performance of VF in direct complex IIR filter design is illustrated by two examples run in the MATLAB 7.1 environment on a 512-RAM 1.8-GHz PC.

4.1 Example 1

In this example, we design a single-passband positive passband filter (PPF), which is widely used in communication systems (e.g. single-side-band communication [1]). The specification is extracted from [2]. The response is sampled at 40 linearly spaced points in the passband, and 80 uniform sampling points in each stopband. The passband spans $[-10, 10]$.

Vector fitting constrains the numerator and denominator of the transfer function to have the same order. An 8-pole (8-zero) complex IIR filter was designed via VF to fit the prescribed response. It takes 0.9063 seconds for the system poles to attain convergence in 5 pole refining iterations. The frequency response and the passband group delay (the change of phase) are shown in Fig. 2. It can be observed that VF achieves an excellent fitting to both desired magnitude and phase response. The L_2 norm and L_∞ norm errors in magnitude of solution are summarized in Table 1. The numerical example is compared with [2], and is shown by Fig. 2. It can be concluded that the phase response matches the desired constant group delay (i.e. linear passband) with a significantly improved computation complexity and better approximation in the

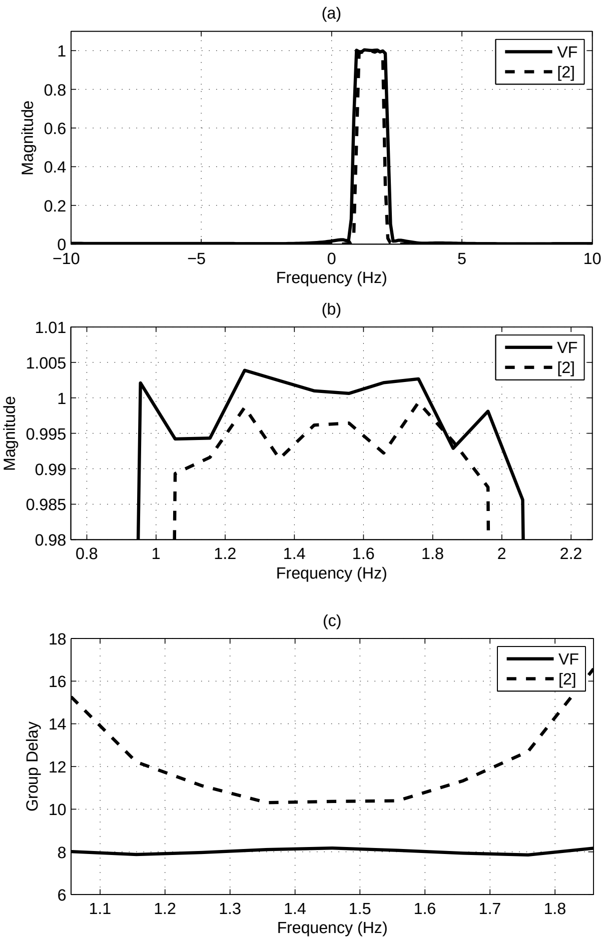

Figure 2: Frequency response of Example 1. (a) Magnitude in the entire band, (b) magnitude in the passband and (c) group delay in the passband.

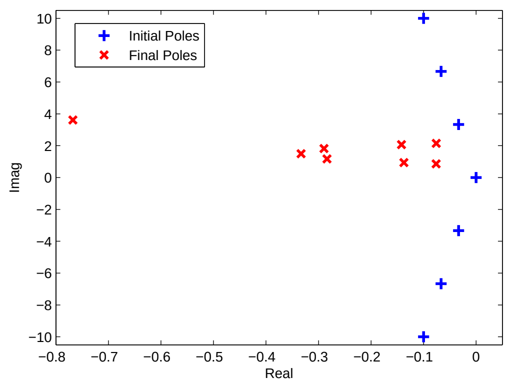

Figure 3: Initial pole placement and final pole locations in Example 1.

passband, with a slightly better stopband design. Fig. 3 shows the initial and final system poles.

4.2 Example 2

The second example demonstrates the versatility of the VF algorithm through the design of a wide-frequency-range double-passband complex filter, which can be used in low-IF architecture [1]. The specifications are as follows:

$$H_d(e^{j\omega}) = \begin{cases} -60\ dBe^{j\omega D}, & (-10f_s \le \omega \le -7f_s) \\ 0\ dBe^{j\omega D}, & (-6f_s \le \omega \le -4f_s) \\ -60\ dBe^{j\omega D}, & (-3f_s \le \omega \le f_s) \\ 0\ dBe^{j\omega D}, & (2f_s \le \omega \le 6f_s) \\ -60\ dBe^{j\omega D}, & (7f_s \le \omega \le -10f_s) \end{cases} \tag{15}$$

where D is the group delay. To illustrate the capability of VF to design wide frequency range filters, we take f_s in the GHz. Uniform sampling points of 80 and 40 are used in each passband and stopband respectively, i.e., 280 sampling points in total. The transition bands are not sampled as a way of relaxation. We set the group delay to be 10 microseconds in both the passband and stopband. To approximate the desired response, a $20th$-order IIR filter is designed via the VF algorithm with the numerical enhancements in Section 3.1. The set of system poles converges in only 4 iterations, taking 0.8063 seconds for computation. From Fig. 4 and Table 1, the complex IIR filter via VF matches the desired magnitude response and phase linearity well over a wide frequency range. The location of initial assigned poles and converged poles in the s-plane is plotted in Fig. 5. It is noticeable that the poles are roughly located separately into two elliptical regions, each of them corresponding to a passband. Fig. 6 shows the L_2 error and the condition number in (3) during each iteration. Both quantities show a significant descending trend for each iteration and converge within a few iterations, and in fact converge much faster than the original VF. It also shows the numerical improvement using row scaling technique.

Acknowledgment

This work was supported in part by the Hong Kong Research Grants Council and the University Research Committee of The University of Hong Kong.

5 Conclusions

This paper has generalized VF to the design of arbitrary response complex IIR continuous-time filters. Without symmetry constraints, the proposed method demonstrates its efficacy in producing low-order approximation functions to the desired magnitude responses over a wide frequency range with matching of phase linearity. Arbitrary response approximation, passband phase matching,

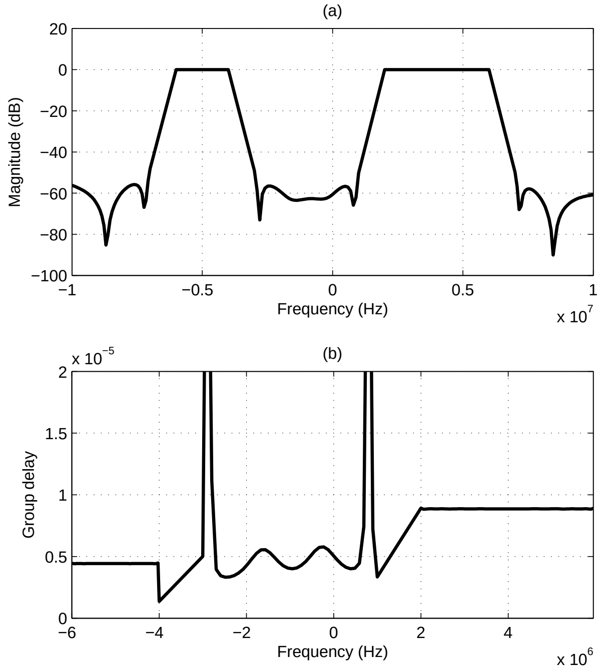

Figure 4: Frequency response of Example 2. (a) Magnitude, (b) Group delay in passband.

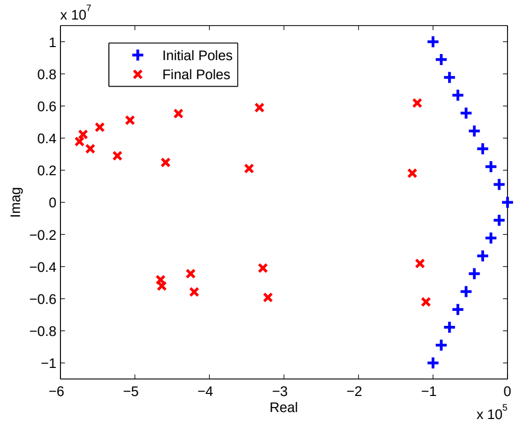

Figure 5: Initial pole placement and final pole locations in Example 2.

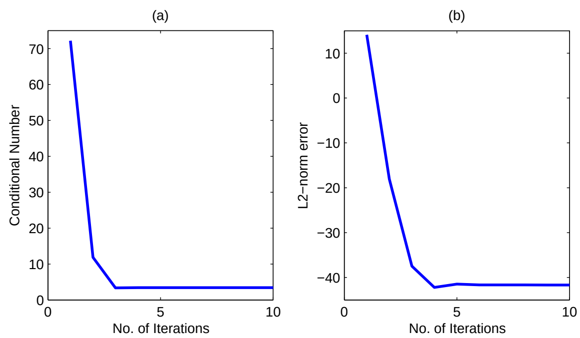

Figure 6: Numerical information for each iteration in Example 2. (a) Conditional number and (b) L_2 error.

and the algorithm effectiveness are definite advantages over existing methods. Different enhancement techniques are applied in the numerical computation. Numerical examples have confirmed the superiority of VF over conventional complex IIR filter design algorithms.

References

[1] K. W. Martin, "Complex signal processing is not complex," *IEEE Trans. Circuits Syst. I*, vol. 51, no. 9, pp. 1823–1836, 2004.

[2] K. W. Martin, "Approximation of complex IIR bandpass filters without arithmetic symmetry," *IEEE Trans Circuits Syst. I*, vol. 52, no. 4, pp. 794–803, Apr. 2005.

[3] J. Mahattanakul and P. Khumsat, "Structure of complex elliptic Gm-C filters suitable for fully differential implementation," *IEE Proceedings - Circuits, Devices and Systems*, vol. 1, no. 4, pp. 275–282, Aug. 2007.

[4] B. Pandita and K. W. Martin, "Designing Complex delta-sigma Modulators with Signal-Transfer Functions having Good Stop-Band Attenuation," in *Proc. IEEE Symp. Circuits and Systems*, May 2007, pp. 3626–3629.

[5] A. Krukowski and I. Kate, "DSP system design: complexity reduced IIR filter implementation for practical application," 2003.

[6] M. A. Teplechuk and J. I. Sewell, "Approximation of arbitrary complex filter responses and their realisation in log domain," *IEE Proceedings - Circuits, Devices and Systems*, vol. 153, no. 6, pp. 583–590, Dec. 2006.

[7] B. Gustavsen and A. Semlyen, "Rational approximation of frequency domain responses by vector fitting," *IEEE Trans. Power Delivery*, vol. 14, no. 3, pp. 1052–1061, July 1999.

[8] B. Gustavsen, "Wide band modeling of power transformers," *IEEE Trans. Power Delivery*, vol. 19, no. 1, pp. 414–422, Jan. 2004.

[9] E. P. Li, E. X. Liu, L. W. Li, and M. S. Leong, "A coupled efficient and systematic full-wave time-domain macromodeling and circuit simulation method for signal integrity analysis of high-speed interconnects," *IEEE Trans. Antennas Propagat.*, vol. 27, no. 1, pp. 213–223, Feb. 2004.

[10] N. Wong and C. Lei, "FIR filter approximation by IIR filters based on discrete-time vector fitting," in *Proc. IEEE Symp. Circuits and Systems*, May 2007, pp. 2343–2346.

[11] W. Hendrickx and T. Dhaene, "A discussion of "Rational approximation of frequency domain responses by vector fitting"," *IEEE Trans. Power Syst.*, vol. 21, no. 1, pp. 441–443, Feb. 2006.

[12] C. Sanathanan and J. Koerner, "Transfer function synthesis as a ratio of two complex polynomials," *IEEE Trans. Automat. Contr.*, vol. 8, no. 1, pp. 56–58, Jan. 1963.

[13] B. Gustavsen, "Improving the pole relocating properties of vector fitting," *IEEE Trans. Power Delivery*, vol. 21, no. 3, pp. 1587–1592, July 2006.

[14] D. Deschrijver, M. Schoeman, T. Dhaene, and P. Meyer, "Experimental analysis on the relaxation of macromodeling methods," in *Proc. IEEE Africon conference*, Sept. 2007.

[15] D. Deschrijver, B. Haegeman, and T. Dhaene, "Orthonormal vector fitting: A robust macromodeling tool for rational approximation of frequency domain responses," *IEEE Trans. Adv. Packag.*, vol. 30, no. 2, pp. 216–225, May 2007.

[16] Y. S. Mekonnen and J. E. Schutt-Aine, "Broadband macromodeling of sampled frequency data using z-domain vector-fitting method," in *Proc. IEEE workshop on sig. prop. on interconnects*, May 2007.

[17] G. H. Golub and C. F. V. Loan, *Matrix Computations*, 3rd ed. London: Johns-Hopkins, 1996.

[18] T. Kobayashi and S. Imai, "Design of IIR digital filters with arbitrary log magnitude function by WLS techniques," *IEEE Trans. Signal Processing*, vol. 38, no. 2, pp. 247–252, Feb. 1990.